

# Polarization-dependent GaN surface grating reflector for short wavelength applications

Joonhee Lee<sup>1</sup>, Sungmo Ahn<sup>1</sup>, Hojun Chang<sup>1</sup>, Jaehoon Kim<sup>2</sup>, Yeonsang Park<sup>3</sup>, and Heonsu Jeon<sup>1,2,4\*</sup>

<sup>1</sup>Department of Physics and Astronomy & Inter-university Semiconductor Research Center, Seoul National University, Seoul 151-747, Korea

<sup>2</sup>Advanced Institutes of Convergence Technology, Suwon 443-270, Korea

<sup>3</sup>Institut des Nanotechnologies de Lyon (INL), INSA de Lyon, 69621 Villeurbanne, France

<sup>4</sup>Department of Biophysics and Chemical Biology, Seoul National University, Seoul 151-747, Korea  
\*hsjeon@snu.ac.kr

**Abstract:** This study proposes a one-dimensional sub-wavelength grating structure on GaN surface which behaves as a reflector for transverse-electric polarized light in the blue wavelength range. The rigorous coupled-wave analysis method was used to analyze the effects of various structural parameters on the reflectance spectra of the grating. Based on the optimal design, a GaN surface grating reflector (SGR) was fabricated using holographic lithography and dry etching processes. It showed reflectance that exceeded 90% over a 60-nm bandwidth. The obtained experimental results were in good agreement with simulated ones. The SGR has an advantage of structural simplicity, which should greatly facilitate the fabrication and integration of high reflectors on GaN-based short-wavelength photonic devices.

©2009 Optical Society of America

**OCIS codes:** (050.1950) Diffraction gratings; (090.1970) Diffractive optics; (160.6000) Semiconductor materials; (220.4241) Nanostructure fabrication.

---

## References and links

1. G. Huang, T. Lu, H. Yao, H. Kuo, S. Wang, C. Lin, and L. Chang, "Crack-free GaN/AlN distributed Bragg reflectors incorporated with GaN/AlN superlattices grown by metalorganic chemical vapor deposition," *Appl. Phys. Lett.* **88**(6), 061904 (2006).
2. S. Park, J. Kim, H. Jeon, T. Sakong, S. Lee, S. Chae, Y. Park, C. Jeong, G. Yeom, and Y. Cho, "Room-temperature GaN vertical-cavity surface-emitting laser operation in an extended cavity scheme," *Appl. Phys. Lett.* **83**(11), 2121–2123 (2003).
3. M. C. Y. Huang, Y. Zhou, and C. J. Chang-Hasnain, "A surface-emitting laser incorporating a high-index-contrast subwavelength grating," *Nat. Photonics* **1**(2), 119–122 (2007).
4. J. Kim, D. Kim, J. Lee, H. Jeon, Y. Park, and Y. Choi, "AlGaIn membrane grating reflector," *Appl. Phys. Lett.* **95**(2), 021102 (2009).
5. S. Goeman, S. Boons, B. Dhoedt, K. Vandeputte, K. Caekebeke, P. Van Daele, and R. Baets, "First demonstration of highly reflective and highly polarization selective diffraction gratings (GIRO-gratings) for long-wavelength VCSEL's," *IEEE Photon. Technol. Lett.* **10**(9), 1205–1207 (1998).
6. M. G. Moharam, and T. K. Gaylord, "Rigorous coupled-wave analysis of planar-grating diffraction," *J. Opt. Soc. Am.* **71**(7), 811–818 (1981).
7. M. G. Moharam, E. B. Grann, D. A. Pommet, and T. K. Gaylord, "Formulation for stable and efficient implementation of the rigorous coupled-wave analysis of binary gratings," *J. Opt. Soc. Am. A* **12**(5), 1068–1076 (1995).
8. E. Bisailon, D. Tan, B. Faraji, A. Kirk, L. Chrowstowski, and D. V. Plant, "High reflectivity air-bridge subwavelength grating reflector and Fabry-Perot cavity in AlGaAs/GaAs," *Opt. Express* **14**(7), 2573–2582 (2006).
9. Y. Ding, and R. Magnusson, "Band gaps and leaky-wave effects in resonant photonic-crystal waveguides," *Opt. Express* **15**(2), 680–694 (2007).
10. S. Boutami, B. Benbakir, X. Letartre, J. L. Leclercq, P. Regreny, and P. Viktorovitch, "Ultimate vertical Fabry-Perot cavity based on single-layer photonic crystal mirrors," *Opt. Express* **15**(19), 12443–12449 (2007).
11. R. Magnusson, and M. Shokooh-Saremi, "Physical basis for wideband resonant reflectors," *Opt. Express* **16**(5), 3456–3462 (2008).
12. M. Bass and Optical Society of America, *Handbook of optics*, 2nd ed. (McGraw-Hill, New York, 1995).
13. R. Wood, "On a remarkable case of uneven distribution of light in diffraction grating problems," *Philos. Mag.* **4**, 396–402 (1902).

14. L. Rayleigh, "Note on the remarkable case of diffraction spectra described by Prof. Wood," *Philos. Mag.* **14**, 60–65 (1907).
  15. E. Popov, M. Neviere, B. Gralak, and G. Tayeb, "Staircase approximation validity for arbitrary-shaped gratings," *J. Opt. Soc. Am. A* **19**(1), 33–42 (2002).
  16. C.-O. Cho, J. Jeong, J. Lee, H. Jeon, I. Kim, D. Jang, Y. Park, and J. Woo, "Photonic crystal band edge laser array with a holographically generated square-lattice pattern," *Appl. Phys. Lett.* **87**(16), 161102 (2005).
  17. C.-O. Cho, J. Lee, Y. Park, Y. Roh, H. Jeon, and I. Kim, "Photonic Crystal Cavity Lasers Patterned by a Combination of Holography and Photolithography," *IEEE Photon. Technol. Lett.* **19**(8), 556–558 (2007).
  18. J. Lee, S. Ahn, S. Kim, D. U. Kim, H. Jeon, S. J. Lee, and J. H. Baek, "GaN light-emitting diode with monolithically integrated photonic crystals and angled sidewall deflectors for efficient surface emission," *Appl. Phys. Lett.* **94**(10), 101105 (2009).
- 

## 1. Introduction

A reflector is an important part in various photonic devices, especially in vertical-cavity surface-emitting lasers (VCSELs) and resonant-cavity light-emitting diodes (RCLEDs). Typically used reflectors are metal mirrors composed of metallic element such as silver or aluminum, or semiconductor distributed Bragg reflectors (DBRs), which consist of periodic layers of two kinds of semiconductors with different refractive indices. For III-nitride system, however, metal mirrors do not provide sufficient reflectivity due to their significant light absorption at short wavelengths. Semiconductor DBRs are also difficult to realize due to the large lattice mismatch and small index contrast between GaN and AlN: Large lattice mismatch requires a special technique in growth, while small index contrast results in an abnormally thick DBR film [1]. Dielectric DBRs can be an alternative [2]. In this case, however, neither electrical injection nor thermal management becomes trivial.

Recently, it has been reported that membrane-type grating reflectors (MGRs) with a sub-wavelength period were integrated onto infrared VCSELs [3]. Our research group also realized AlGaIn sub-wavelength MGR [4], which could be a solution circumventing the aforementioned limitations of conventional reflector approaches for III-nitride system. However, since the MGRs are constructed to a membrane structure in which grating layer is clad by low refractive index materials (most frequently, the air) on both sides, they are not ready yet for electrically injected devices and suffer from the lack of mechanical rigidity.

In this study, we demonstrate that a high reflector can still be made simply by engraving a sub-wavelength grating on GaN surface, similarly to the case of the GaAs and InP grating reflectors for near-infrared [5]. This should greatly facilitate to design and fabricate GaN-based photonic devices that require reflectors. The rigorous coupled-wave analysis (RCWA) method [6,7] and the finite-difference time-domain (FDTD) method were used to find an optimal design of the surface grating reflector (SGR) and to assess their performance characteristics. Based on the optimized structural design, a GaN SGR was fabricated on a large area using holographic lithography. The measured reflectance spectra are presented and compared with simulation results.

## 2. Design and simulation

Sub-wavelength period MGRs show high reflectance over a broad wavelength range. They use the guided-mode resonance phenomenon that involves the coupling between a quasi-guided or leaky waveguide mode along the membrane and its 0th order diffraction into the outer space [8–11]. For the case of the SGRs discussed in this paper, on the other hand, there is no apparent guided mode in the lateral directions. Nonetheless, it was reported that such a surface grating still can exhibit high reflectivity when light is incident to the grating from the substrate side [5]. It must be stressed that, in most light-emitting devices, light is generated inside semiconductor material and emitted to outside. Considering the structural simplicity in comparison with MGRs, therefore, SGRs should be of high practicality and of great importance for light-emitting devices application.

An intuitive explanation for highly reflective characteristic of the SGRs can be given as follows. When light impinges vertically onto the grating, it diffracts into different directions, depending on the wavelength and the grating period. If all the diffractions except for the 0th order can be suppressed effectively, then the incident light either reflects or transmits in the

surface-normal direction. Moreover, the lights passing through the grating peaks and troughs should interfere destructively if the phase difference between them is  $\pi$  in radians. By choosing the grating height and the filling factor appropriately, therefore, all energy can be made reflected back with zero transmittance. Due to the one-dimensional (1D) nature, the grating is inherently polarization-dependent in its reflection/transmission characteristics.

For GaN SGR, it is assumed that the transverse-electric (TE; electric field direction parallel to the grating lines) polarized light is incident from the GaN side in the direction normal to the air/GaN interface plane, as shown in Fig. 1. The optimum structure was designed to maximize the 0th order reflection at  $\lambda = 450$  nm, using the RCWA method. Because there is no established design rule for the SGRs yet, the optimal structure was determined through repeated calculations near the values based on the aforementioned intuitive principle, which can be expressed as  $\Lambda \approx \lambda$ ,  $h \approx \lambda/2(n_{\text{GaN}} - n_{\text{air}})$ , and  $F \approx 0.5$ , where  $\Lambda$  and  $h$  are the grating period and height while  $F$  is the GaN filling factor.

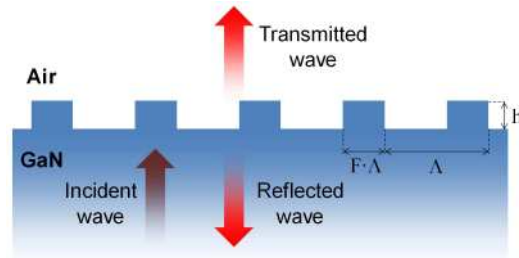


Fig. 1. Schematic diagram of a 1D GaN SGR.

After detailed calculation with various structural parameters, we determined the optimized structure, for which  $\Lambda = 419$  nm,  $h = 114$  nm, and  $F = 0.4$ . Figures 2(a) and 2(b) show the diffraction efficiency spectra of the optimized structure for the TE and transverse-magnetic (TM) polarizations, respectively, which are calculated by the RCWA method. It was assumed that the refractive index dispersion of GaN is given by the Sellmeier equation [12], its value at the target wavelength  $\lambda = 450$  nm being 2.49.

As shown in Fig. 2(a), the diffraction efficiency of the 0th order reflection reaches the unity at  $\lambda = 450$  nm, which indicates that the surface grating indeed operates as a good reflector for TE-polarized light. It should be noted that the high order diffractions are indeed suppressed effectively, as required in our previous intuitive discussion. For the optimized structure, the reflectance  $R$  is greater than 0.8 over the spectral bandwidth of  $\Delta\lambda_R \approx 90$  nm ( $\Delta\lambda_R / \lambda \approx 0.2$ ) and greater than 0.9 for  $\Delta\lambda_R \approx 60$  nm ( $\Delta\lambda_R / \lambda \approx 0.13$ ); those reflectance bandwidths are broader than the typical gain bandwidth of the InGaN quantum wells ( $\Delta\lambda_{PL} \approx 30$  nm). It should be also mentioned that the RCWA calculations correctly produce the *Rayleigh anomaly* at the wavelength equal to the grating period [13-14]. Below the critical wavelength, the first order transmission suddenly becomes available and electromagnetic field energy has to be rearranged accordingly among the available diffraction orders.

The electric field distribution calculated with the FDTD method is depicted in Fig. 2(c), where  $\lambda = 450$  nm TE-polarized plane wave propagates upwards from below. The electric field is strongly concentrated at the grating peaks and troughs; but their phases are shifted by  $\pi$  from each other. Hence, they interfere destructively in the exit medium and very little electromagnetic energy can be transmitted beyond the grating. In Fig. 2(d), we plot electric field profiles integrated over the regions of a grating peak and trough. This clearly confirms our intuitive explanation that the out-of-phase condition between the lights passing the grating peaks and troughs is responsible for the high reflection of the SGR. It is worth noting that the total electric field disappears almost instantaneously beyond the grating.

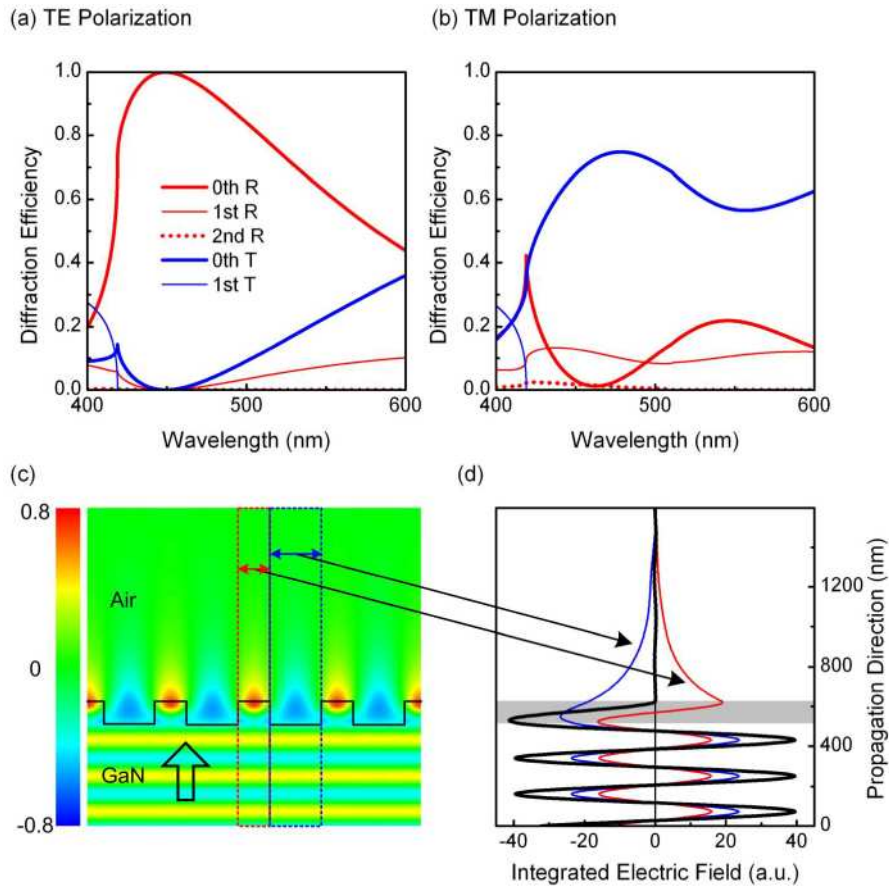


Fig. 2. Calculated diffraction efficiency spectra of a GaN SGR (optimized for  $\lambda = 450$  nm and TE-polarization) for all the allowed diffraction orders in both reflection and transmission: (a) TE-polarization and (b) TM-polarization. Light is incident in the normal direction from the GaN side. (c) Electric field distribution in the vicinity of the SGR for the  $\lambda = 450$  nm TE-polarized light. (d) Electric field profiles integrated over a grating peak (red line) and over a grating trough (blue line), and their sum (black line). Shaded is the grating region.

As far as the actual fabrication process is concerned, however, accurate realization of the nanostructures as designed is very difficult. To investigate the fabrication tolerance of the SGR, the influences of various structural parameters on the reflectance were examined. Shown in Fig. 3 are the reflectance (to be more accurate, the 0th order reflected diffraction efficiency) spectra plotted as a function of the grating period, height, filling factor, and slanted angle. For each contour plot, the parameters other than the one under investigation are assumed to be the optimized values. Figure 3(a) indicates that, as the grating period increases, the reflectance band moves to a longer wavelength region while its maximum reflectance remains almost the same. As for the grating height shown in Fig. 3(b), there is a broad region around the optimized height ( $h = 114$  nm), in which reflectance is maintained at a high level. On the other hand, high reflectance is well preserved as long as the filling factor remains less than 0.4, as shown in Fig. 3(c). It decreases dramatically, however, when the factor exceeds 0.45. These findings imply that the filling factor is the most sensitive and important parameter in SGR fabrication.

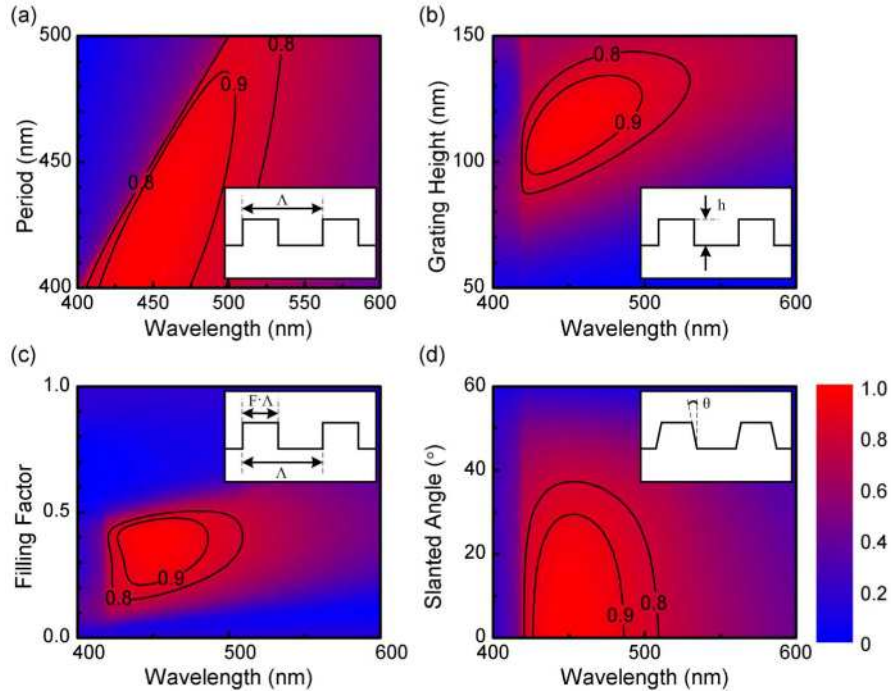


Fig. 3. Contour plots of the GaN SGR (optimized for  $\lambda = 450$  nm TE-polarization) for various structural parameters: (a) period, (b) height, (c) filling factor, and (d) slanted angle of the grating.

It is extremely difficult to fabricate gratings with vertical sidewalls by dry etching process, which is partly due to the mechanical hardness of GaN. So we calculated the reflectance of the grating with various slanted sidewall angles. In this calculation, the angled grating of a smooth profile was considered as a stack of rectangular gratings, the GaN filling factor at the mid height of the stack being the optimized value of  $F = 0.4$ . For sufficient accuracy in the RCWA calculation, we approximated the slanted grating using 50-step staircase, in which the thickness of each slice (2.28 nm) was much thinner than wavelength ( $\lambda = 450$  nm) [15]. Figure 3(d) shows however that the influence of the slanted angle on the reflectance is insignificant. For example, a grating with  $10^\circ$  angled sidewall exhibits the reflectance spectrum that is practically unchanged from that of the  $0^\circ$  sidewall grating. These simulation results imply that the structural tolerance range is sufficiently large; hence, a GaN SGR with high reflectance can be fabricated without difficulty as far as the filling factor is suitably controlled.

### 3. Fabrication and measurements

A 4.5- $\mu\text{m}$ -thick GaN layer was grown on a double-sided polished c-plane sapphire wafer using a metal-organic chemical-vapor-deposition technique. Holographic lithography, which used the interference of two coherent laser beams, was employed to generate 1D grating patterns on a sample typically as large as  $1 \times 1$   $\text{cm}^2$ .

As far as the fabrication of periodic nanostructures is concerned, holographic lithography has advantages over electron-beam lithography in processing time and cost. Our group previously fabricated highly functional nanophotonic devices using this technique [16–18]. Figure 4(a) shows a schematic diagram of the holographic lithography setup used in this study. A 325-nm He-Cd laser beam illuminates the sample stage after expanded by the spatial filter: Two beams, one directly incident onto a sample and the other reflected from a mirror installed at the right angle to the sample plane, interfere to produce 1D grating patterns on the

sample surface. The grating period is controlled conveniently by rotating the sample stage to vary the beam incidence angle.

After the successive depositions of SiO<sub>2</sub> and Cr hard mask layers on GaN using plasma-enhanced chemical-vapor-deposition and e-gun evaporation techniques, a grating was patterned on photoresist (PR) using holographic lithography. The PR patterns were then transferred to the Cr and SiO<sub>2</sub> layers sequentially by reactive-ion-etching (RIE) and finally to the GaN layer by inductively-coupled-plasma RIE. Figures 4(b) and 4(c) show scanning electron microscope (SEM) images of the fabricated SGR. The parameters determined from the images are  $\Lambda \sim 425$  nm,  $h \sim 126$  nm,  $F \sim 0.4$ , and  $\theta \sim 10^\circ$ . These are reasonably close to the optimum values and are within the fabrication tolerance limits suggest in Fig. 3. Thus, the high reflectance can be expected to result as simulated.

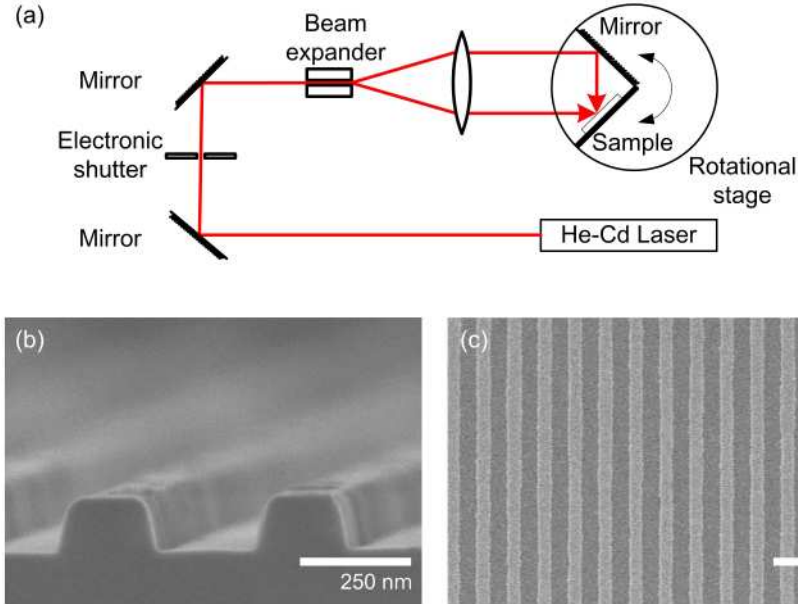


Fig. 4. (a) Schematic diagram of the holographic lithography setup used in the experiments. SEM images of the fabricated GaN SGR: (b) cross-section and (c) plan-view.

The reflectance spectra of the GaN grating were measured. As shown in Fig. 5(a), white light from a 1 kW Xe lamp was incident to the grating through the sapphire substrate. A combination of pinhole and polarizer allowed us to illuminate the grating over a probing area of  $\sim 1$  mm<sup>2</sup> with well-defined polarization beam. Light reflected from the grating was fed into a spectrometer to record its spectral characteristics. Measured reflectance spectra were then normalized using a protected Al mirror (PAV-PM-1025C, CVI Melles Griot, USA).

Figure 5(b) shows the measured and calculated reflectance spectra for the entire GaN grating structure including the sapphire substrate. In order to accurately account for the refractive index dispersions of GaN and sapphire, we used the Sellmeier equations given in the literature [12]. The overall measured reflectance spectra were in excellent agreement with the RCWA results. This indicates that, despite the wildly corrugated surface condition, a simple but properly designed 1D GaN surface grating can serve as a good reflector. We attribute the small spectral red-shift to the slight discrepancy of the actual grating period ( $\Lambda \sim 425$  nm) from the designed value ( $\Lambda = 419$  nm). The rapid oscillations simply originate from the Fabry-Pérot cavity across the thin GaN film.

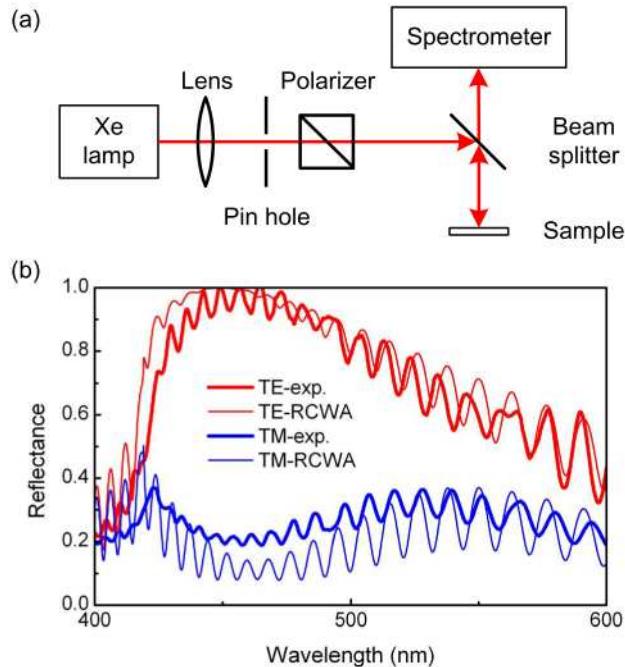


Fig. 5. (a) Schematic of the reflectance spectrum measurement setup, where the Xe lamp is used as a white light source. (b) Experimental and calculated reflectance spectra of the SGR (but including the sapphire substrate) for both TE and TM polarizations.

We also performed an independent confirmation experiment. We employed lasers (He-Cd, Ar, and frequency-doubled Nd:YAG lasers) to measure the reflectivity directly at a few selected wavelengths ( $\lambda = 442$  nm, 514 nm, and 532 nm). The results were in accordance with theoretical values: The reflectance at  $\lambda = 442$  nm was as high as  $R \approx 0.92$ , while  $R \sim 0.8$  at  $\lambda = 514$  nm and 532 nm. Although it is desirable to measure the reflectance of the SGR itself, it is difficult (if not totally impossible) to physically isolate the SGR in the form of free-standing GaN thin film. Nevertheless, from the experimental results and the comparison with theoretical predictions, we are quite confident that the GaN SGR we fabricated has the reflectance characteristics very close to the theoretical one shown in Fig. 2(a). The developed GaN SGR is therefore ready to be integrated in actual GaN-based photonic devices where high reflections are required.

#### 4. Conclusion

We have investigated GaN surface gratings in an effort to develop reflectors for GaN-based photonic devices operating at short wavelengths. Through RCWA and FDTD calculations, we found and confirmed the optimal structure that exhibits high reflectance ( $R > 0.9$ ) for TE-polarized light over a wide spectral range ( $\Delta\lambda_R \approx 60$  nm) centered at  $\lambda = 450$  nm. It was also verified that the GaN SGR has generous structural tolerance: Accordingly, extreme precision in fabrication is not a requisite. Using simple holographic lithography and dry etching techniques, GaN SGRs were fabricated over a large area at high throughput. The experimental results were shown to be in good agreement with the reflectance spectra obtained by the RCWA simulation. The submicron-period GaN SGRs developed in this study should have an impact on a variety of GaN-based photonic devices operating in the blue or UV region.

### **Acknowledgements**

This work was supported by the IT R&D program of MKE/KEIT [2009-F-025-01, Development of Core Technology for High Efficiency Light Emitting Diode based on New Concepts], and also in part by the Seoul R&BD program. The authors thank S.-J. Lee and J. H. Baek at Korea Photonics Technology Institute for providing GaN epilayers.